Biochemistry and Cell Biology
Biochimie et biologie cellulaire

Reduced miR-144-3p expression in serum and bone mediates osteoporosis pathogenesis by targeting RANK

SCHOLARONE™
Manuscripts

1   **Reduced *miR-144-3p* expression in serum and bone mediates osteoporosis**

2   **pathogenesis by targeting RANK**

3

4   Chunqing Wang[1], Hanliang He[1], Liang Wang[1], Yu Jiang[1], Youjia Xu[1]

5

6

7   [1]Department of Orthopaedics, The Second Affiliated Hospital of Soochow University,

8   1055 Sanxiang Road, Suzhou 215004, China

9

10

11

12

13

14

15

16

17

18   **Corresponding author: Youjia Xu**

19   Email: xuyoujia@medmail.com.cn

20   Telephone: +86-0512-67783346

21   Fax: +86-0512-67783346

22

23

1

24   **Abstract**

25   Osteoblasts and osteoclasts are responsible for the formation and resorption of

26   bone, respectively. An imbalance between these two processes results in a disease

27   called osteoporosis, in which a decreased level of bone strength increases the risk of a

28   bone fracture. MicroRNAs (miRNAs) are small non-coding RNA molecules of 18–25

29   nucleotides that have been previously shown to control bone metabolism by

30   regulating osteoblast and osteoclast differentiation. In the present study, we detected

31   the expression pattern of 10 miRNAs in patient serum samples, and identified six

32   miRNAs altered expression in patients with osteoporosis relative to non-osteoporosis.

33   We selected *miR-144-3p* for further investigation, and showed that it regulates

34   osteoclastogenesis by targeting *RANK* and that it is conserved amongst vertebrates.

35   Disrupted expression of *miR-144-3p* in CD14+ PBMCs changed TRAP activity and

36   the osteoclast-specific genes *TRAP*, *cathepsin K (CTSK)*, and *NFATC.* TRAP staining，

37   CCK-8 and flow cytometry analyses revealed that *miR-144-3p* also affects osteoclast

38   formation, proliferation and apoptosis. Together, these results indicate that

39   *miR-144-3p* critically mediates bone homeostasis, and thus, represents a promising

40   novel therapeutic candidate for the treatment of this disease.

41

42   **Keywords:** osteoporosis, *miR-144-3p*, *RANK*, osteoclastogenesis

43

44

45   **Introduction**

46   The maintenance of bone homeostasis requires the correct balance between

47   osteogenesis and bone resorption, as mediated by osteoblasts and osteoclasts,

48   respectively (BENNETT *et al.* 2005) (MULARI *et al.* 2004). Imbalance between these

49   two processes results in osteoporosis, which is characterized by a decrease in bone

50   mineral density and by abNon-osteoporosis bone microarchitecture (BOLLERSLEV *et*

51   *al.* 2005; LI *et al.* 2010). As life expectancy increases worldwide, a greater number of

52   individuals suffer from osteoporosis; for example, almost half of the population in

53   China is affected by the condition, and affected individuals suffer an average fracture

54   ratio of almost 33% (WANG *et al.* 2015; ROUSE *et al.* 2016). Despite extensive

55   research, the underlying mechanisms for this disease, and novel osteoporosis therapies,

56   remain elusive (ADLER 2016).

57   Osteoclasts critically mediate bone building by enabling bone resorption (AMANO

58   *et al.* 1998). The OPG/RANKL/RANK signalling pathway was recently identified as

59   a classical pathway associated with osteoclast differentiation (WRIGHT *et al.* 2009).

60   The pathway includes the receptor activator of the nuclear factor kappa-B (NF-κB)

61   ligand (RANKL), which is an osteoclast differentiation factor and receptor of the

62   receptor activator of NF-κB (RANK) (SOBACCHI *et al.* 2007). RANK is located in the

63   cell membrane of osteoclasts, and functions to accelerate osteoclast activation and

64   differentiation (HSU *et al.* 1999). Osteoprotegerin (OPG), also known as

65   osteoclastogenesis inhibitory factor (OCIF) or tumour necrosis factor receptor

66   superfamily member 11B (TNFRSF11B), is a decoy receptor that binds RANKL, and

67   thereby prevents RANK-mediated NF-κB activation (BOYCE and XING 2007). A

3

68   recent study successfully induced circulating CD14+ peripheral blood mononuclear

69   cells (CD14+ PBMCs), which are early osteoclast progenitors, to differentiate into

70   osteoclasts *in vitro* by activating either macrophage colony-stimulating factor (M-CSF)

71   or RANKL (SHALHOUB *et al.* 2000; SORENSEN *et al.* 2007). This was possible because

72   CD14+ PBMCs express RANK, which is activated by binding RANKL and

73   subsequently induces osteoclast differentiation (HSU *et al.* 1999).

74   MicroRNAs (miRNAs) are a class of small noncoding single stranded RNAs

75   composed of 18–25 nucleotides (BARTEL 2004), which were first identified in *C.*

76   *elegans*, but that have now been reported to play various crucial roles in cell

77   development, proliferation, and differentiation (EBERT and SHARP 2012; MENDELL

78   and OLSON 2012). Each miRNA regulates a given target gene by recognizing a 'seed

79   sequence' site, (located in either the 3′ untranslated region (3′UTR) or coding

80   sequence (CDS) of the target gene), to promote degradation or inhibit translation of

81   the target gene (RANA 2007; PAL *et al.* 2015). Recent research revealed that miRNA

82   activity mediates bone homeostasis by regulating the expression of key osteoblast and

83   osteoclast differentiation genes (VAN WIJNEN *et al.* 2013). For instance, *miRNA-145*

84   targets *Sp7* to suppress osteogenic differentiation (JIA *et al.* 2013), *miR-21* has been

85   reported to mediate mesenchymal stem cell (MSC) proliferation and differentiation

86   during bone formation (ZHAO *et al.* 2015), and similarly, *miR-214* targets *FGFR1* to

87   attenuate osteogenic MSC differentiation (SHI *et al.* 2013). miRNAs have also been

88   shown to affect osteoclast function, for example, overexpression and silencing of

89   *miR-503* in CD14+ PBMCs was recently found to inhibit and promote

4

90 RANK-induced osteoclastogenesis, respectively, via the targeting of RANK (CHEN *et*

91 *al.* 2014). In contrast, miRNAs are themselves targets of many regulators that affect

92 bone differentiation. For instance, *DLX3* is a crucial regulator of hair follicle

93 differentiation and cycling, but also targets *miR-124* in bone tissue to negatively

94 regulate osteoclastic differentiation (ZHAO *et al.* 2016). Thus, miRNAs have been

95 identified to regulate bone homeostatic processes, and in fact, the importance and

96 complexity of this miRNA network suggests that continued research is required to

97 elucidate the extent to which it affects osteoporosis pathogenesis.

98   In the clinical setting, diagnosis of osteoporosis was predominantly achieved by

99 measuring bone mineral density and bone quality, where a loss of bone mineral

100 density is indicative of osteoporosis. Early diagnosis is beneficial in facilitating an

101 optimal treatment regime. Serum or systemically circulating miRNAs have been

102 described in many diseases, including many types of cancer, as well as myocardial

103 conditions, endometriosis, gastrointestinal disease, and/or diabetes mellitus (DEVAUX

104 *et al.* 2015). Various miRNAs have been previously reported as serum biomarkers for

105 osteoporosis; for example, Seeliger *et al.* reported *miRNA-21*, *-23a*, *-24*, *-25*, *-100*,

106 and *-125b* to be expressed at a significantly higher level in the serum and bone tissues

107 of patients with osteoporosis as compared to healthy individuals (SEELIGER *et al.*

108 2014). Very recently, Chen *et al.* described 15 serum miRNAs that were differentially

109 expressed in OVX rats (an osteoporosis animal model), as identified and validated by

110 microarray analysis and quantitative real-time PCR (qRT-PCR) (CHEN *et al.* 2016).

111 Taken together, these previous studies suggest that miRNAs are promising biomarkers

5

112 for the early diagnosis of osteoporosis.

113   In the present study, we used qRT-PCR to reveal that *miR-144-3p* is

114 downregulated in osteoporotic serum and bone tissues, and thus is a likely biomarker

115 for the diagnosis of osteoporosis. We also identified conserved *miR-144-3p* target sites

116 in the *RANK* 3′UTR via bioinformatics analysis, and demonstrated that

117 overexpression of *miR-144-3p* inhibited *RANK* expression *in vitro* to mediate

118 osteoclast formation, proliferation, and apoptosis. Thus, we conclude that *miR-144-3p*

119 targets osteoclasts via *RANK*. Our research provides a novel candidate biomarker for

120 the diagnosis of osteoporosis in the clinical setting.

121

122 **Materials and Methods**

123 **Primary human samples**

124   Recruited patients admitted to our clinic with hip fractures were separated into

125 two groups, comprising patients with osteoporosis who had a fracture (subject group),

126 and patients non-osteoporosis but who had a fracture (control group). Blood and bone

127 samples were collected during implantation of a total endoprosthesis or gamma nail

128 into the proximal femur. The Local Ethical Review Committee of The Second

129 Affiliated Hospital of Soochow University approved the present study.

130

131 **Sample processing, miRNA extraction, and qRT-PCR**

132   miRNAs from serum were extracted using the miRNeasy Serum/Plasma Kit

133 (Qiagen), according to the manufacturer's instructions. miRNA and mRNA were

6

134   extracted from bone tissue using TRIzol, as per the manufacturer's instructions.

135   miRNA was subsequently transcribed to generate cDNA using the PrimeScript^{TM} One

136   Step cDNA Synthesis Kit (Takara), and mRNA was transcribed to first strand cDNA

137   using the First Strand cDNA Synthesis Kit (Takara) for gene expression analysis in

138   bone tissue. qRT-PCR was performed using the ABI 7000 RT-PCR system (ABI,

139   USA), with the listed primers (Table 1) and PrimeScript^{TM} RT reagent kit (Takara,

140   Japan), according to the manufacturer's instructions.

141

142   **CD14+ PBMC cultures**

143   Whole blood was obtained using a protocol approved by the Local Research

144   Ethics Committee, and PBMCs were isolated as previously described (SORENSEN *et al.*

145   2007). CD14+ PBMCs were purified using CD14 antibody-coated magnetic cell

146   sorting (MACS) MicroBeads (Miltenyi Biotec), and the purity of these cells was

147   assessed using flow cytometry. When the CD14+ PBMCs purity was more than 90%,

148   subsequent experiments were carried out. CD14+ PBMCs (density 2.5×10^5

149   cells/well, in a 48-well cluster plate) were cultured (37 °C, in a humidified

150   atmosphere with 5% CO_2) in alpha minimum essential medium (a-MEM)

151   supplemented with 10% foetal bovine serum (FBS), penicillin (50 IU/mL), and

152   streptomycin (50 mg/mL). Osteoclastic differentiation was induced by replacing this

153   medium with that supplemented with 25 ng/mL recombinant M-CSF and 25 ng/mL

154   human RANKL (R&D Systems, Minneapolis).

155

Luciferase activity assay

156

157   A segment of the wild type (WT) *RANK* 3′UTR cloned into the pMir-reporter

158   vector (Ambion), and a mutant *RANK* 3′UTR was generated by altering the predicted

159   *miR-144-3p RANK* 3′UTR binding site via a two-step PCR approach. HEK 293T cells

160   were co-transfected with either a WT or mutant *RANK* 3′ UTR reporter vector, and the

161   *miR-144-3p* mimic or negative control constructs, cultured for 24 h, and then assessed

162   to ascertain their exhibited luciferase activity using a dual-luciferase reporter assay

163   system (Promega).

Tartrate-resistant acid phosphatase (TRAP) staining

164

165   TRAP staining was performed using a commercially available TRAP staining kit

166   according to the manufacturer's instructions (Sigma). Osteoclasts were identified as

167   TRAP-positive multinucleated (more than or equal to three nuclei) cells. The number

168   of TRAP-positive multinucleated giant cells were counted in a 48-well culture plate

169   using a Leica DM4000B microscope and photographed using a Leica DFC450c

170   camera.

171

Cell proliferation assay

172

173   Cell proliferation was analysed using the Cell Counting Kit 8 (CCK-8; Dojindo).

174   After 6 days, CD14+ PBMCs were inducible, differently treated cells were then

175   incubated for another 24 h. The optical density (OD) of each group was measured at

176   450 nm using a BioTek microplate reader.

177

8

178

Cell apoptosis assay

179

180 CD14+ PBMC apoptosis was analysed via the flow cytometry method (FCM),

181 using an Annexin V-PI Apoptosis Detection Kit (Abcam). Briefly, cells were collected

182 six days after the induction of differentiation, washed with phosphate-buffered saline

183 (PBS), and suspended in 500 µl of binding buffer. They were then incubated (37℃,

184 10 min) with Annexin V, stained with propidium iodide (PI), and analysed via the

185 FCM to determine their relative quantitative rate of apoptosis.

186

Statistical analyses

187

188 Data are presented as the mean ± SD. Statistical differences between two or more

189 groups were determined using the Student's t-test and one-way ANOVA followed by

190 Student–Newman–Keuls test, respectively. All experiments were repeated at least

191 three times, and representative results are shown. A p-value <0.05 was considered to

192 indicate statistical significance.

193

194

Results

195

qRT-PCR screening of differential miRNA expression in serum and bone samples

196

of patients with and without osteoporosis

197

198 We selected 10 candidate miRNAs, which were reportedly related to bone

199 metabolism, to undergo qRT-PCR analysis to examine their differential expression in

9

200   serum and bone samples of patients with and without osteoporosis (Fig. 1A).15

201   non-osteoporosis and 45 osteoporosis sample was used. The non-osteoporosis sample

202   we label with Non-osteoporosis and osteoporosis patient label with osteoporosis in the

203   next experiments. All the sample clinic data was provided in the supplementary. The

204   results of this analysis showed no difference in *miRNA-7-5p* or *miR-211-5p* expression,

205   but a significant upregulation of *miR-24-3p*, *27a-3p*, *100*, *125b*, and *122a* expressions

206   in both the serum and bone samples of osteoporosis with as compared to

207   non-osteoporosis. The expression of *miR-128* was found to be upregulated in bone

208   tissue, but unchanged in the serum of osteoporosis with as compared to without

209   non-osteoporosis. Conversely, *miR-145* was upregulated only in the serum but not the

210   bone tissue of osteoporosis. While *miR-144-3p* has not been previously reported to be

211   associated with osteoporosis, the results of the present study show that it was

212   significantly downregulated in both the serum and bone samples of patients with as

213   compared to non-osteoporosis (Fig. 1B, C). Thus, the generated data clearly

214   demonstrate differential miRNA expression in osteoporosis, as compared to those not

215   affected by the disease.

216

217   ***miRNA-144-3p* mediates gene expression in osteoporosis**

218   We selected *miR-144-3p* as the focus for our subsequent analyses investigating

219   the effects of miRNA activity on the pathogenesis of osteoporosis. We first used

220   TargetScan online software (http://www.targetscan.org/vert-71/) to predict

221   *miR-144-3p* targets and refined the resultant list to include only those candidate genes

10

222   associated with bone metabolism; the list comprised of *BMPR1A*, *COL11A*, *SMAD4*,

223   *ESRRG,* and *RANK*. To investigate the expression patterns of these candidate genes,

224   total mRNA was extracted from patient samples and subjected to qRT-PCR. The

225   results of this analysis showed that *BMPR1A*, *COL11A,* and *ESRRG* expression was

226   unchanged between patients with and without osteoporosis (Fig 2A, B, D); however,

227   the expression of *SMAD4* and *RANK* was significantly upregulated in patients with

228   osteoporosis as compared to those without the disease (Fig 1C, E). A previous report

229   demonstrated that *miR-144-3p* regulates osteogenic differentiation, as well as the

230   proliferation of murine MSCs by specifically targeting *Smad4*; thus, we selected

231   *RANK* to be the focus of our subsequent analyses. We used ELISA to examine the

232   RANK content in patient serum samples, and resultantly showed that the

233   concentration of RANK was significantly higher in patients with osteoporosis than in

234   those without osteoporosis (Fig 1F). This suggests that *RANK* concentration is

235   regulated by *miR-144-3p*.

236

237   **RANK is a direct *miR-144-3p* target gene**

238   TargetScan online software was used to identify a probable single *miR-144-3p*

239   target site in the *RANK* 3′UTR that was comprised of nine nucleotides homologous

240   with the *miR-144-3p* consensus seed sequence. Furthermore, this *RANK* 3′UTR

241   *miR-144-3p* target site was found to be conserved in humans, chimps, mice, dogs, and

242   lizards (Fig 3A).

243   To investigate the potential differential expression of *miR-144-3p* during

244 osteoclastogenesis, CD14+ PBMCs from patients unaffected by osteoporosis were

245 induced to differentiate via M-CSF and RANKL treatment. These cells were cultured

246 for 6 days, and then analysed via qRT-PCR to determine their *miR-144-3p* expression.

247 The results of this analysis showed that the CD14+ PBMC *miR-144-3p* expression

248 was significantly downregulated in response to the induction of differentiation as

249 compared to undifferentiated cells (at 0 days) (Fig 3A). The *miR-144-3p* negative

250 control, inhibitor, and mimic were next transfected into CD14+ PBMCs, which were

251 subsequently induced to differentiate via treatment with M-CSF and RANKL, and

252 collected after 6 days of culture. qRT-PCR analysis of *RANK* expression at this point

253 revealed it to be increased and decreased in the inhibitor- and mimic-transfected cells,

254 respectively, compared with the negative control-transfected cells (Fig 3C). These

255 data suggest that *RANK* is a *miR-144-3p* target in CD14+ PBMCs.

256   To validate this hypothesis, we cloned a WT and mutant (seed sequence) *RANK*

257 3′UTR into the pMir-reporter vector to generate a CMV-luciferase-WT and

258 CMV-luciferase-mutant *RANK* 3′UTR expression vector, respectively (Fig 3D).

259 Dual-luciferase reporter assays were then conducted by co-transfecting HEK 293T

260 cells with these expression vectors and the *miR-144-3p* negative control, mimic,

261 and/or inhibitor. The results of these analyses showed that luciferase activity was

262 significantly decreased in response to co-transfection of the CMV-luciferase-WT

263 *RANK* 3′UTR and *miR-144-3p* mimic, as compared to co-transfection of the

264 CMV-luciferase-WT *RANK* 3′UTR and the *miR-144-3p* negative control. In contrast,

265 co-transfection of the CMV-luciferase-mutant *RANK* 3′UTR and *miR-144-3p* mimic

12

266   failed to inhibit luciferase activity (Fig 3E). Similarly, western blot analysis of RANK

267   protein levels in CD14+ PBMCs transfected with the *miR-144-3p* negative control,

268   inhibitor, and/or mimic showed RANK production to be increased and decreased in

269   response to transfection of the *miR-144-3p* inhibitor and mimic, respectively, as

270   compared to RANK levels in the negative control (Fig 3F). Together, these data

271   confirm *RANK* as a *miRNA-144-3p* target.

272

273   ***miR-144-3p* regulates the osteoclastogenesis of CD14+ PBMCs following M-CSF**

274   **and RANKL treatment**

275   To investigate the role of *miRNA-144-3p* during osteoclastogenesis, CD14+

276   PBMCs from a patient unaffected by osteoporosis were transfected with the

277   *miR-144-3p* negative control, mimic, and/or inhibitor, treated with M-CSF and

278   RANKL, cultured for 6 days, and then analysed to evaluate their expression of the

279   osteoclast-specific genes *TRAP*, cathepsin K *(CTSK)*, and *NFATC*, and for their

280   exhibited TRAP activity. The results of these analyses showed that treating the

281   CD14+ PBMCs with the *miR-144-3p* mimic and inhibitor significantly decreased and

282   increased TRAP activity, respectively, as compared with the negative control (Fig 4A).

283   Similarly, the qRT-PCR analysis demonstrated that *TRAP*, *CTSK*, and *NFATC* mRNA

284   expression was down- and up-regulated in response to treating the CD14+ PBMCs

285   with the *miR-144-3p* mimic and inhibitor, respectively, as compared to treating them

286   with the negative control (Fig 4B–D). These results suggest that *miR-144-3p*

287   negatively regulates osteoclastogenesis.

13

288 ***miR-144-3p* affects osteoclast formation following the M-CSF and RANKL**

289 **treatment of CD14+ PBMCs**

290 To explore the role of *miR-144-3p* in osteoclast formation, TRAP staining

291 experiments were performed. The results showed that the number of TRAP-positive

292 cells decreased in the *miR-144-3p* mimic group, and the number of TRAP-positive

293 cells increased in the *miR-144-3p* inhibitor group as compared with the negative

294 control group (Fig. 5A B). These results demonstrated that *miR-144-3p* affects

295 osteoclast formation.

296

297

298 ***miR-144-3p* mediates the proliferation and apoptosis of M-CSF/RANKL-induced**

299 **osteoclasts**

300 To investigate the role of *miR-144-3p* in cell proliferation and apoptosis during

301 osteoclastogenesis, CD14+ PBMCs were transfected with the *miRNA-144-3p* negative

302 control, inhibitor, and/or mimic, and induced to differentiate via treatment with

303 M-CSF and RANKL. These cells were cultured for 6 days, and then subjected to

304 CCK-8 assay and flow cytometric analysis (Fig 5A). The results of the CCK-8 assay

305 revealed that treatment with the *miR-144-3p* mimic and inhibitor reduced and

306 increased CD14+ PBMC proliferation, respectively, as compared to treatment with the

307 negative control (Fig 5B). Similarly, the results of the flow cytometric analysis

308 showed that transfection of the *miR-144-3p* mimic increased CD14+ PBMC apoptosis

309 as compared to transfection with the negative control; however, no difference was

14

310   observed in response to transfecting CD14+ PBMCs with the *miR-144-3p* inhibitor

311   (Fig 5C). Together, these data indicate that *miR-144-3p* mediates apoptosis and cell

312   proliferation during osteoclastogenesis.

313

314   **Discussion**

315   Osteoporosis is a disorder characterised by a loss of balance between osteoblast

316   and osteoclast activities (LI *et al.* 2010). An increasing proportion of aging individuals

317   worldwide are affected by this condition; thus, study into novel therapeutic

318   interventions is urgently required to mitigate the increasing medical and

319   socioeconomic burden caused by osteoporosis (WANG *et al.* 2015). miRNAs critically

320   mediate osteoporosis pathogenesis, and many previous studies have revealed that this

321   occurs via their exerted effects on both osteoblasts and osteoclasts (VAN WIJNEN *et al.*

322   2013). In the present study, we identified *miR-144-3p* as an osteoporosis-associated

323   miRNA that targets *RANK* to mediate osteoclastogenesis, and whose differential

324   expression likely contributes to the pathogenesis of this disease.

325

326   ***miR-144-3p* is a novel serum biomarker for osteoporosis**

327   Extensive research into the use of serum-based miRNAs as disease biomarkers

328   has been conducted over the last several years (DEVAUX *et al.* 2015; ROUSE *et al.*

329   2016). Furthermore, various osteoporosis miRNA biomarkers have been investigated

330   as potential diagnostic tools in the clinical setting (MENG *et al.* 2015). For example, in

331   2014, Seeliger *et al.* reported five freely circulating serum and bone tissue-contained

332   miRNAs (*miR-21*, *23a*, *24*, *25*, *100,* and *125b*) that were associated with osteoporotic

333   fractures (SEELIGER *et al.* 2014), and more recently, Chen *et al.* identified 15 serum

334   miRNA osteoporosis biomarkers (CHEN *et al.* 2016). Meng *et al.* and Zat *et al.*

335   identified *miR-194-5p* and *miR-422a*, respectively, as potential biomarkers for

336   postmenopausal osteoporosis (CAO *et al.* 2014; MENG *et al.* 2015), and similarly,

337   Wang *et al.* reported *miR-133a* in human circulating monocytes as an additional

338   candidate biomarker associated with postmenopausal osteoporosis (WANG *et al.*

339   2012).

340   In the present study, we selected and assessed the expression of 10 miRNAs in

341   patients with osteoporosis, two of which (*miR-100* and *miR-125b*) were previously

342   evaluated by Seeliger *et al.* (SEELIGER *et al.* 2014). The results of the present study are

343   consistent with those of Seeliger *et al*., which showed that both *miR-100* and

344   *miR-125b* were upregulated in patients with osteoporosis. *miR-122a* was also found in

345   the present study to be upregulated in both the serum and bone samples of patients

346   with, as compared to Non-osteoporosis. Conversely, *miR-128* and *miR-145a* were

347   shown to be elevated only in the bone and serum samples, respectively, of patients

348   with osteoporosis. Of these, *miR-145a* has been previously shown to suppress

349   osteogenic differentiation by targeting *Sp7* (JIA *et al.* 2013). In the present study, we

350   found *miR-144-3p* to be differentially expressed in osteoporotic serum and bone

351   samples, suggesting that it is a promising novel biomarker for the diagnosis of

352   osteoporosis in the clinical setting. Although many miRNAs have, to date, been

353   identified as candidate osteoporosis biomarkers, their effect on osteoporosis

354   pathogenesis is not well understood。

RANK is a direct target of *miRNA-144-3p*

356   miRNAs regulate gene expression by recognising the 3′UTR or CDS of various

357   target genes (BARTEL 2004). Of these target genes, *SMAD4* and *RANK* were

358   established to exhibit differential expression in patients with osteoporosis via

359   qRT-PCR. We selected *RANK* for further analysis, since *SMAD4* has been previously

360   reported to be targeted by *miR-144-3p* during its regulation of murine MSC

361   osteogenic differentiation and proliferation (HUANG *et al.* 2016). RANK exists in the

362   cell membrane, and after binding to its ligand, mediates osteoclast differentiation. Our

363   loss-of-function and overexpression experiments revealed that RANK is a target gene

364   for *miR-144-3p*.

miR-144-3p targets *RANK* to regulate osteoclastogenesis

366   *miR-144-3p* regulates osteoclastogenesis by targeting *RANK*. This was shown in

367   the present study with both loss-of-function and overexpression experiments for

368   *miR-144-3p in vitro*. As a known type II membrane protein and a member of the

369   tumour necrosis factor (TNF) superfamily (BOYCE and XING 2007; WRIGHT *et al.*

370   2009), RANKL induces osteoclast differentiation by binding and activating RANK in

371   myeloid-lineage cells (BOYCE and XING 2007; BOYCE and XING 2008). RANK may

372   also bind to OPG, which is a protein secreted predominantly by cells of the osteoblast

373   lineage that potently inhibits osteoclast formation by preventing the binding of

374   RANKL to RANK (WRIGHT *et al.* 2009). In the present study, we revealed that

375   *miR-144-3p* inhibits TRAP activity. It is well established that the bone matrix

17

376   phosphoproteins osteopontin and bone sialoprotein are highly efficient *in vitro* TRAP

377   substrates that bind to osteoclasts when phosphorylated (HAYMAN 2008). Furthermore,

378   TRAP activity has been previously shown to be an osteoclast marker (HALLEEN *et al.*

379   2006; WU *et al.* 2009), and increased TRAP activity is considered to be indicative of a

380   high rate of osteoclast differentiation. In the present study, we also examined the

381   expression of two key genes, *NFATC1* and *CTSK*, in PBMCs after the transfection

382   with the *miR-144-3p* mimic and inhibitor. *NFATC1* is involved in the NFATC1

383   signalling pathway, which is critical to the regulation of osteoclast differentiation and

384   maturation (CROTTI *et al.* 2006; KIM and KIM 2014). CTSK has been shown to be

385   predominantly involved in degrading the organic bone matrix and controlling

386   osteoclast population size by regulating apoptosis (HENRIKSEN *et al.* 2006; FULLER *et*

387   *al.* 2008). In the present study, transfection of the *miR-144-3p* mimic and inhibitor

388   induced a significant decrease and increase, respectively, in the expression of both

389   *NFATC1* and *CTSK*. Furthermore, transfection of both constructs affected cell

390   proliferation and apoptosis, strongly suggesting that *miR-144-3p* affects

391   osteoclastogenesis by targeting *RANK*.

392   The results of the present study also identified *SMAD4* as being differentially

393   expressed in response to modulating *miRNA-144-3p* expression. *SMAD4* is known to

394   be activated by BMP signalling and to predominantly mediate osteoblastogenesis. In

395   fact, a recent study showed that *miRNA-144-3p* could target *SMAD4* to regulate

396   osteoblastogenesis (HUANG *et al.* 2016); thus, *miR-144-3p* appears to not only

397   participate in osteoclastogenesis, but also osteoblastogenesis.

18

398   In summary, we conclude from the results of the present study that *miR-144-3p*

399   should be considered as a serum osteoporosis biomarker for use in the clinical setting.

400   *miR-144-3p* via direct targeting of *RANK* mediates osteoclastogenesis. Thus,

401   *miRNA-144-3p* may be a promising novel therapeutic candidate for the treatment

402   osteoporosis.

403

404   **Acknowledgments**

408

409   **Conflict of interest**

410   All authors have no conflicts of interest.

411   **References**

412   Adler, R. A., 2016 Osteoporosis treatment: complexities and challenges. J Endocrinol Invest 39**:**
413   719-720.
414   Amano, H., S. Yamada and R. Felix, 1998 Colony-stimulating factor-1 stimulates the fusion process in
415   osteoclasts. J Bone Miner Res 13**:** 846-853.
416   Bartel, D. P., 2004 MicroRNAs: genomics, biogenesis, mechanism, and function. Cell 116**:** 281-297.
417   Bennett, C. N., K. A. Longo, W. S. Wright, L. J. Suva, T. F. Lane *et al.*, 2005 Regulation of
418   osteoblastogenesis and bone mass by Wnt10b. Proc Natl Acad Sci U S A 102**:** 3324-3329.
419   Bollerslev, J., S. G. Wilson, I. M. Dick, F. M. Islam, T. Ueland *et al.*, 2005 LRP5 gene polymorphisms
420   predict bone mass and incident fractures in elderly Australian women. Bone 36**:** 599-606.
421   Boyce, B. F., and L. Xing, 2007 Biology of RANK, RANKL, and osteoprotegerin. Arthritis Res Ther 9 Suppl
422   1**:** S1.
423   Boyce, B. F., and L. Xing, 2008 Functions of RANKL/RANK/OPG in bone modeling and remodeling. Arch
424   Biochem Biophys 473**:** 139-146.
425   Cao, Z., B. T. Moore, Y. Wang, X. H. Peng, J. M. Lappe *et al.*, 2014 MiR-422a as a potential cellular
426   microRNA biomarker for postmenopausal osteoporosis. PLoS One 9**:** e97098.
427   Chen, C., P. Cheng, H. Xie, H. D. Zhou, X. P. Wu *et al.*, 2014 MiR-503 regulates osteoclastogenesis via

428   targeting RANK. J Bone Miner Res 29**:** 338-347.

429   Chen, J., K. Li, Q. Pang, C. Yang, H. Zhang *et al.*, 2016 Identification of suitable reference gene and
430   biomarkers of serum miRNAs for osteoporosis. Sci Rep 6**:** 36347.

431   Crotti, T. N., M. Flannery, N. C. Walsh, J. D. Fleming, S. R. Goldring *et al.*, 2006 NFATc1 regulation of the
432   human beta3 integrin promoter in osteoclast differentiation. Gene 372**:** 92-102.

433   Devaux, Y., M. Mueller, P. Haaf, E. Goretti, R. Twerenbold *et al.*, 2015 Diagnostic and prognostic value
434   of circulating microRNAs in patients with acute chest pain. J Intern Med 277**:** 260-271.

435   Ebert, M. S., and P. A. Sharp, 2012 Roles for microRNAs in conferring robustness to biological
436   processes. Cell 149**:** 515-524.

437   Fuller, K., K. M. Lawrence, J. L. Ross, U. B. Grabowska, M. Shiroo *et al.*, 2008 Cathepsin K inhibitors
438   prevent matrix-derived growth factor degradation by human osteoclasts. Bone 42**:** 200-211.

439   Halleen, J. M., S. L. Tiitinen, H. Ylipahkala, K. M. Fagerlund and H. K. Vaananen, 2006 Tartrate-resistant
440   acid phosphatase 5b (TRACP 5b) as a marker of bone resorption. Clin Lab 52**:** 499-509.

441   Hayman, A. R., 2008 Tartrate-resistant acid phosphatase (TRAP) and the osteoclast/immune cell
442   dichotomy. Autoimmunity 41**:** 218-223.

443   Henriksen, K., M. G. Sorensen, R. H. Nielsen, J. Gram, S. Schaller *et al.*, 2006 Degradation of the
444   organic phase of bone by osteoclasts: a secondary role for lysosomal acidification. J Bone
445   Miner Res 21**:** 58-66.

446   Hsu, H., D. L. Lacey, C. R. Dunstan, I. Solovyev, A. Colombero *et al.*, 1999 Tumor necrosis factor
447   receptor family member RANK mediates osteoclast differentiation and activation induced by
448   osteoprotegerin ligand. Proc Natl Acad Sci U S A 96**:** 3540-3545.

449   Huang, C., J. Geng, X. Wei, R. Zhang and S. Jiang, 2016 MiR-144-3p regulates osteogenic differentiation
450   and proliferation of murine mesenchymal stem cells by specifically targeting Smad4. FEBS
451   Lett 590**:** 795-807.

452   Jia, J., Q. Tian, S. Ling, Y. Liu, S. Yang *et al.*, 2013 miR-145 suppresses osteogenic differentiation by
453   targeting Sp7. FEBS Lett 587**:** 3027-3031.

454   Kim, J. H., and N. Kim, 2014 Regulation of NFATc1 in Osteoclast Differentiation. J Bone Metab 21**:**
455   233-241.

456   Li, W. F., S. X. Hou, B. Yu, M. M. Li, C. Ferec *et al.*, 2010 Genetics of osteoporosis: accelerating pace in
457   gene identification and validation. Hum Genet 127**:** 249-285.

458   Mendell, J. T., and E. N. Olson, 2012 MicroRNAs in stress signaling and human disease. Cell 148**:**
459   1172-1187.

460   Meng, J., D. Zhang, N. Pan, N. Sun, Q. Wang *et al.*, 2015 Identification of miR-194-5p as a potential
461   biomarker for postmenopausal osteoporosis. PeerJ 3**:** e971.

462   Mulari, M. T., Q. Qu, P. L. Harkonen and H. K. Vaananen, 2004 Osteoblast-like cells complete
463   osteoclastic bone resorption and form new mineralized bone matrix in vitro. Calcif Tissue Int
464   75**:** 253-261.

465   Pal, M. K., S. P. Jaiswar, V. N. Dwivedi, A. K. Tripathi, A. Dwivedi *et al.*, 2015 MicroRNA: a new and
466   promising potential biomarker for diagnosis and prognosis of ovarian cancer. Cancer Biol Med
467   12**:** 328-341.

468   Rana, T. M., 2007 Illuminating the silence: understanding the structure and function of small RNAs.
469   Nat Rev Mol Cell Biol 8**:** 23-36.

470   Rouse, R., B. Rosenzweig, K. Shea, A. Knapton, S. Stewart *et al.*, 2016 MicroRNA biomarkers of
471   pancreatic injury in a canine model. Exp Toxicol Pathol.

472   Seeliger, C., K. Karpinski, A. T. Haug, H. Vester, A. Schmitt *et al.*, 2014 Five freely circulating miRNAs and
473   bone tissue miRNAs are associated with osteoporotic fractures. J Bone Miner Res 29**:**
474   1718-1728.
475   Shalhoub, V., G. Elliott, L. Chiu, R. Manoukian, M. Kelley *et al.*, 2000 Characterization of osteoclast
476   precursors in human blood. Br J Haematol 111**:** 501-512.
477   Shi, K., J. Lu, Y. Zhao, L. Wang, J. Li *et al.*, 2013 MicroRNA-214 suppresses osteogenic differentiation of
478   C2C12 myoblast cells by targeting Osterix. Bone 55**:** 487-494.
479   Sobacchi, C., A. Frattini, M. M. Guerrini, M. Abinun, A. Pangrazio *et al.*, 2007 Osteoclast-poor human
480   osteopetrosis due to mutations in the gene encoding RANKL. Nat Genet 39**:** 960-962.
481   Sorensen, M. G., K. Henriksen, S. Schaller, D. B. Henriksen, F. C. Nielsen *et al.*, 2007 Characterization of
482   osteoclasts derived from CD14+ monocytes isolated from peripheral blood. J Bone Miner
483   Metab 25**:** 36-45.
484   van Wijnen, A. J., J. van de Peppel, J. P. van Leeuwen, J. B. Lian, G. S. Stein *et al.*, 2013 MicroRNA
485   functions in osteogenesis and dysfunctions in osteoporosis. Curr Osteoporos Rep 11**:** 72-82.
486   Wang, O., Y. Hu, S. Gong, Q. Xue, Z. Deng *et al.*, 2015 A survey of outcomes and management of
487   patients post fragility fractures in China. Osteoporos Int 26**:** 2631-2640.
488   Wang, Y., L. Li, B. T. Moore, X. H. Peng, X. Fang *et al.*, 2012 MiR-133a in human circulating monocytes:
489   a potential biomarker associated with postmenopausal osteoporosis. PLoS One 7**:** e34641.
490   Wright, H. L., H. S. McCarthy, J. Middleton and M. J. Marshall, 2009 RANK, RANKL and osteoprotegerin
491   in bone biology and disease. Curr Rev Musculoskelet Med 2**:** 56-64.
492   Wu, Y., J. W. Lee, L. Uy, B. Abosaleem, H. Gunn *et al.*, 2009 Tartrate-resistant acid phosphatase (TRACP
493   5b): a biomarker of bone resorption rate in support of drug development: modification,
494   validation and application of the BoneTRAP kit assay. J Pharm Biomed Anal 49**:** 1203-1212.
495   Zhao, N., D. Han, Y. Liu, Y. Li, L. Zeng *et al.*, 2016 DLX3 negatively regulates osteoclastic differentiation
496   through microRNA-124. Exp Cell Res 341**:** 166-176.
497   Zhao, W., Y. Dong, C. Wu, Y. Ma, Y. Jin *et al.*, 2015 MiR-21 overexpression improves osteoporosis by
498   targeting RECK. Mol Cell Biochem 405**:** 125-133.

499

500 **Tables**

501 **Table 1** List of primers used in this study

Gene name	Forward primer	Reverse primer	Note
BMPR1A	GCTTCATGGCACTGGGATG	CATCATCTGGACAGTGCCCT	qRT-PCR
COL11A	CACCCTCATTGTTGACTGCA	GGCAGCAACCTCAAAGACTT	qRT-PCR
SMAD4	TGATCTATGCCCGTCTCTGG	CCAGGTGATACAACTCGTTCG	qRT-PCR
ESRRG	GAATGGCCATCAGAACGGAC	CACACTTGGTCTGGGGATCT	qRT-PCR
RANK	ACTACACCAAGTACCTGCGT	ACGAACATGGAGCGGGAG	qRT-PCR
TRAP	ACCAATTCTGTGTCCTCGGA	TAATCGAGTGCAGGGGTTCC	qRT-PCR
NFATC1	GCCCGAAGACTACTCCTCTT	GCTCATGTAGGACGTAGGGG	qRT-PCR
CTSK	TGCAGAAGAACCGGGGTATT	AGGGCTTTCTCATTCCCCTC	qRT-PCR
RANK	TTCCTGGATGTTTGGAAAC	GAGACATGAAGGTGAAGTAC	3'UTR CLONE

502

503

22

504   **Figure legends**

505   **Fig. 1 miRNA expression patterns in bone and serum samples from**

506   **Non-osteoporosis and osteoporosis** **(A)** Selected candidate miRNAs, and

507   corresponding qRT-PCR primer sequences. **(B)** Expression patterns of the selected

508   candidate miRNAs in patient serum samples. **(C)** Expression patterns of the selected

509   candidate miRNAs in patient bone samples. Expression levels are represented as the

510   mean ± S.D, with statistical significance being assessed via the Student's *t*-test

511   (p<0.05).

512

513   **Fig. 2 Potential *miR-144-3p* target genes expression patterns in non-osteoporosis**

514   **and osteoporosis.** Online software was used to predict *miR-144-3p* target genes, and

515   the resultant list of candidates was refined to include only those genes associated with

516   bone homeostasis. Selected candidate genes were verified to be differentially

517   expressed between non-osteoporosis and osteoporosis, via qRT-PCR. **(A–E)** The

518   expression patterns of **(A)** *BMPR1A*, **(B)** *COL11A*, (C) *SMAD4*, **(D)** *ESRRG*, and **(E)**

519   *RANK* in non-osteoporosis and osteoporosis in bone tissue. **(F)** The level of RANK

520   production in patient serum samples was assessed via ELISA. Expression levels are

521   represented as the mean ± S.D., with statistical significance being assessed via the

522   Student's *t*-test (p<0.05).

523

524   **Fig. 3 *RANK* is a *miR-144-3p* target gene (A)** Using TargetScans online software,

525   we identified a *miR-144-3p* target site (red colour) in the *RANK* 3′UTR that is

23

526   conserved in humans, chimps, mice, dogs, and lizards. **(B)** The expression of

527   *miR-144-3p* was measured in CD14+ PBMCs using qRT-PCR, six days after the cells

528   were induced to differentiate. **(C)** CD14+ PBMCs were transfected with the

529   *miR-44-3p* mimic or inhibitor, and their expression of *RANKL* was then assessed via

530   qRT-PCR. **(D)** A WT and mutant *RANKL* 3′UTR was cloned into the pMir-reporter

531   vector to generate the CMV-luciferase-*RANKL* and CMV-luciferase-*RANKL* mutant

532   3′UTR vectors. **(E)** A cell-transfection experiment was performed to demonstrate that

533   *miR-144-3p* inhibits *RANKL* expression *in vivo*. +, added; -, not added. **(F)** Western

534   blot analysis demonstrating that *miR-144-3p* affects RANKL protein levels *in vivo*. +,

535   added; -, not added. Data represent the mean ± S.D., with statistical significance being

536   assessed by the Student's *t*-test (p<0.05).

537

538   **Fig. 4 *miR-144-3p* regulates the induction of CD14+ PBMCs to undergo**

539   **osteoclastogenesis via M-CSF and RANKL treatment (A)** CD14+ PBMCs were

540   induced to differentiate via M-CSF and RANKL treatment and cultured for six days,

541   before they exhibited TRAP activity. Transfection of the *miR-144-3p* mimic and

542   inhibitor was shown to decrease and increase CD14+ PBMC TRAP activity,

543   respectively. **(B–D)** qRT-PCR analysis of **(B)** *TRAP*, **(C)** *NFATC,* and **(D)** *CTSK*

544   mRNA expression in response to transfection of CD14+ PBMCs with the

545   *miRNA-144-3p* negative control, mimic, or inhibitor. Data represent the mean ± S.D.,

546   with statistical significance being assessed by the Student's t-test (p<0.05).

547

548   **Fig. 5 *miR-144-3p* regulates osteoclast formation following the M-CSF and**

549   **RANKL treatment of CD14+ PBMCs.** (A) The cells were induced by the addition

550   of M-CSF+RANKL for 6 days, after which the *miR-144-3p* mimic and inhibitor was

551   added. (B) The statistics of the number of TRAP-positive cells. Statistical significance

552   was assessed using the Student's *t*-test (p<0.05).

553   **Fig. 6 Effects of transfecting CD14+ PBMCs with the *miR-144-3p* mimic,**

554   **inhibitor, or negative control on cell proliferation and apoptosis (A)** A CCK-8

555   assay was performed to evaluate the effect of transfecting CD14+ PBMCs with the

556   *miR-144-3p* mimic, inhibitor, and/or negative control on cell proliferation. **(B)** A

557   statistical analysis of the results revealed that the *miR-144-3p* mimic and inhibitor

558   inhibited and increased CD14+ PBMC proliferation, respectively. **(C)** The effects of

559   *miR-144-3p* mimic, inhibitor, and/or negative control transfection on CD14+ PBMC

560   apoptosis was analysed via flow cytometry. Data represent the mean ± S.D., with

561   statistical significance being assessed by the Student's *t*-test (p<0.05).

A

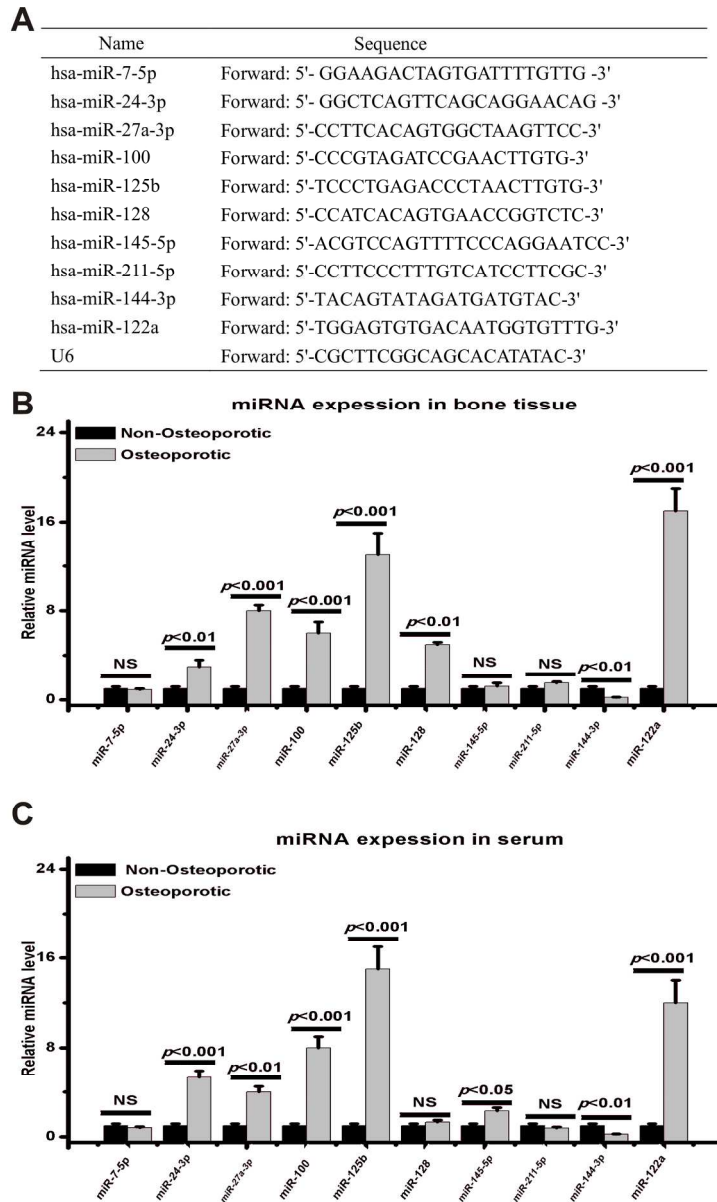| Name	Sequence
hsa-miR-7-5p	Forward: 5'- GGAAGACTAGTGATTTTGTTG -3'
hsa-miR-24-3p	Forward: 5'- GGCTCAGTTCAGCAGGAACAG -3'
hsa-miR-27a-3p	Forward: 5'-CCTTCACAGTGGCTAAGTTCC-3'
hsa-miR-100	Forward: 5'-CCCGTAGATCCGAACTTGTG-3'
hsa-miR-125b	Forward: 5'-TCCCTGAGACCCTAACTTGTG-3'
hsa-miR-128	Forward: 5'-CCATCACAGTGAACCGGTCTC-3'
hsa-miR-145-5p	Forward: 5'-ACGTCCAGTTTTCCCAGGAATCC-3'
hsa-miR-211-5p	Forward: 5'-CCTTCCCTTTGTCATCCTTCGC-3'
hsa-miR-144-3p	Forward: 5'-TACAGTATAGATGATGTAC-3'
hsa-miR-122a	Forward: 5'-TGGAGTGTGACAATGGTGTTTG-3'
U6	Forward: 5'-CGCTTCGGCAGCACATATAC-3'

Fig. 1 miRNA expression patterns in bone and serum samples from Non-osteoporosis and osteoporosis (A) Selected candidate miRNAs, and corresponding qRT-PCR primer sequences. (B) Expression patterns of the selected candidate miRNAs in patient serum samples. (C) Expression patterns of the selected candidate miRNAs in patient bone samples. Expression levels are represented as the mean ± S.D, with statistical significance being assessed via the Student's t-test (p<0.05).
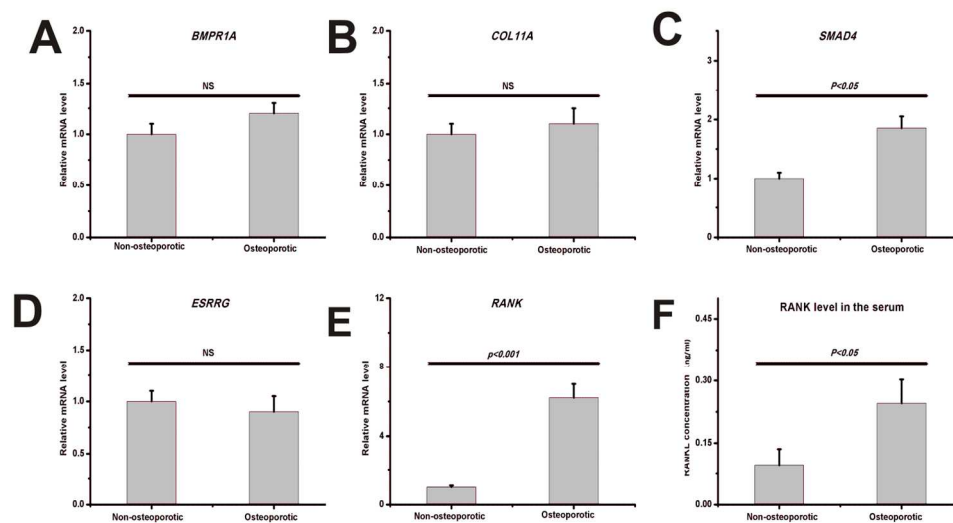
146x233mm (300 x 300 DPI)

Fig. 2 Potential miR-144-3p target genes expression patterns in non-osteoporosis and osteoporosis. Online software was used to predict miR-144-3p target genes, and the resultant list of candidates was refined to include only those genes associated with bone homeostasis. Selected candidate genes were verified to be differentially expressed between non-osteoporosis and osteoporosis, via qRT-PCR. (A–E) The expression patterns of (A) BMPR1A, (B) COL11A, (C) SMAD4, (D) ESRRG, and (E) RANK in non-osteoporosis and osteoporosis in bone tissue. (F) The level of RANK production in patient serum samples was assessed via ELISA. Expression levels are represented as the mean ± S.D., with statistical significance being assessed via the Student's t-test (p<0.05).

139x77mm (300 x 300 DPI)

Fig. 3 RANK is a miR-144-3p target gene (A) Using TargetScans online software, we identified a miR-144-3p target site (red colour) in the RANK 3'UTR that is conserved in humans, chimps, mice, dogs, and lizards. (B) The expression of miR-144-3p was measured in CD14+ PBMCs using qRT-PCR, six days after the cells were induced to differentiate. (C) CD14+ PBMCs were transfected with the miR-44-3p mimic or inhibitor, and their expression of RANKL was then assessed via qRT-PCR. (D) A WT and mutant RANKL 3'UTR was cloned into the pMir-reporter vector to generate the CMV-luciferase-RANKL and CMV-luciferase-RANKL mutant 3'UTR vectors. (E) A cell-transfection experiment was performed to demonstrate that miR-144-3p inhibits RANKL expression in vivo. +, added; -, not added. (F) Western blot analysis demonstrating that miR-144-3p affects RANKL protein levels in vivo. +, added; -, not added. Data represent the mean ± S.D., with statistical significance being assessed by the Student's t-test (p<0.05).
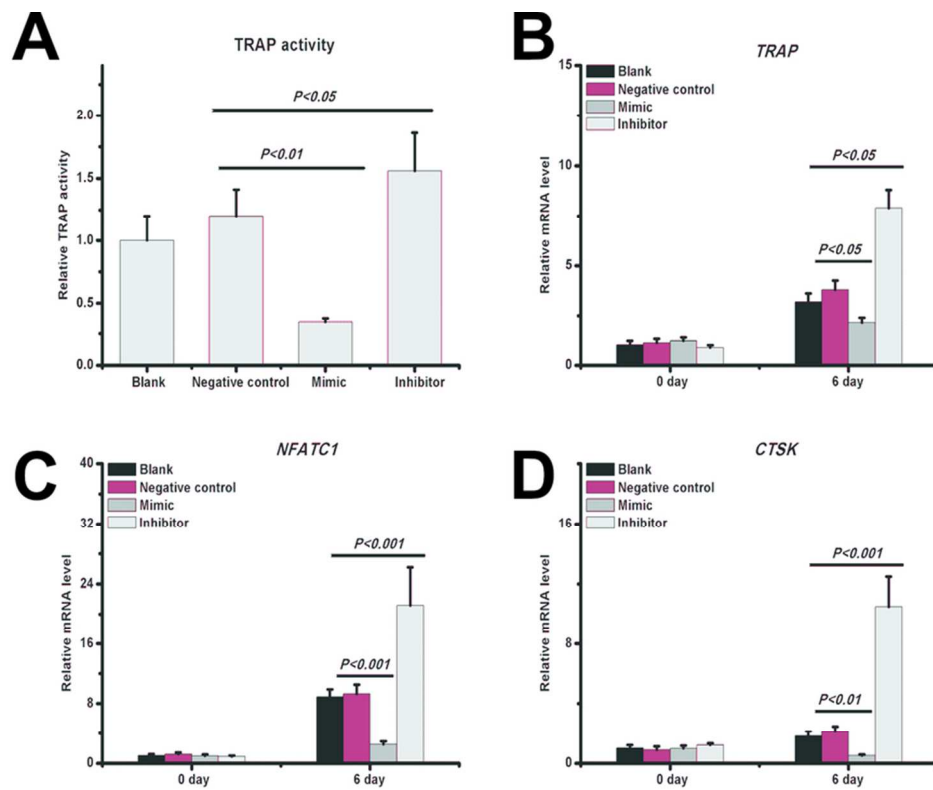
190x98mm (300 x 300 DPI)

Fig. 4 miR-144-3p regulates the induction of CD14+ PBMCs to undergo osteoclastogenesis via M-CSF and RANKL treatment (A) CD14+ PBMCs were induced to differentiate via M-CSF and RANKL treatment and cultured for six days, before they exhibited TRAP activity. Transfection of the miR-144-3p mimic and inhibitor was shown to decrease and increase CD14+ PBMC TRAP activity, respectively. (B–D) qRT-PCR analysis of (B) TRAP, (C) NFATC, and (D) CTSK mRNA expression in response to transfection of CD14+ PBMCs with the miRNA-144-3p negative control, mimic, or inhibitor. Data represent the mean ± S.D., with statistical significance being assessed by the Student's t-test (p<0.05).
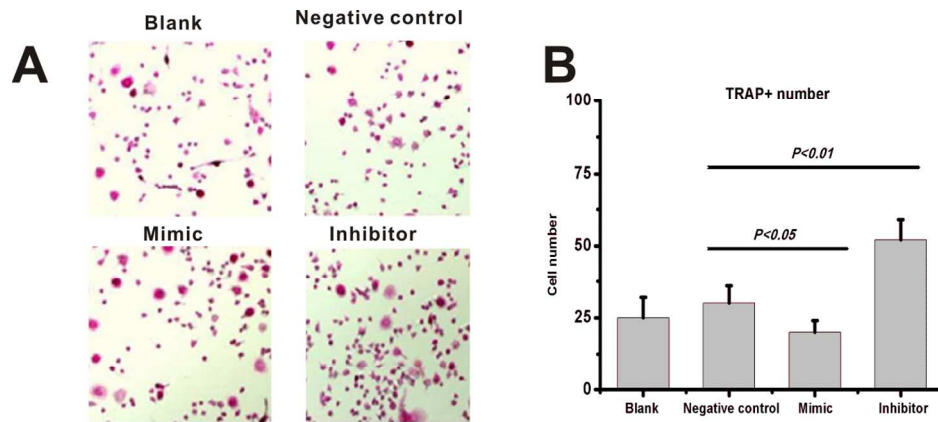
78x64mm (300 x 300 DPI)

Fig. 5 miR-144-3p regulates osteoclast formation following the M-CSF and RANKL treatment of CD14+ PBMCs. (A) The cells were induced by the addition of M-CSF+RANKL for 6 days, after which the miR-144-3p mimic and inhibitor was added. (B) The statistics of the number of TRAP-positive cells. Statistical significance was assessed using the Student's t-test (p<0.05).
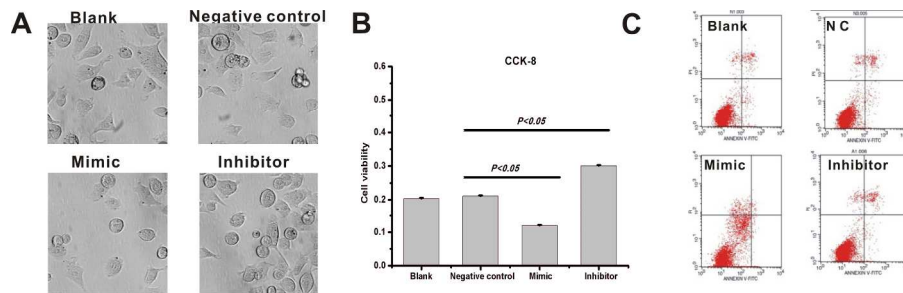
125x56mm (300 x 300 DPI)

Fig. 6 Effects of transfecting CD14+ PBMCs with the miR-144-3p mimic, inhibitor, or negative control on cell proliferation and apoptosis (A) A CCK-8 assay was performed to evaluate the effect of transfecting CD14+ PBMCs with the miR-144-3p mimic, inhibitor, and/or negative control on cell proliferation. (B) A statistical analysis of the results revealed that the miR-144-3p mimic and inhibitor inhibited and increased CD14+ PBMC proliferation, respectively. (C) The effects of miR-144-3p mimic, inhibitor, and/or negative control transfection on CD14+ PBMC apoptosis was analysed via flow cytometry. Data represent the mean ± S.D., with statistical significance being assessed by the Student's t-test (p<0.05).

220x66mm (300 x 300 DPI)